Indonesian Journal of Electrical Engineering and Computer Science
Vol. 3, No. 3, September 2016, pp. 519 ~ 526
DOI: 10.11591/ijeecs.v3.i2.pp519-526

Fission Transmission Linear-to-Circular Polarization Conversion Based on Compact Bi-Layer structure

Farman Ali Mangi[1], Shaoqiu Xiao[1]*, Ghulam Ali Mallah[2], Ghulam Fatima Kakepoto[1], Memon Imran[3]
[1]School of Physical Electronics, University of Electronic Science and Technology of China, Chengdu, 610054, Sichuan, China
[2]Department of Computer Science, Shah Abdul Latif University, Khairpur, Sindh, Pakistan.
[3]College of Computer Science, Zhejiang University, Hangzhou, Zhejiang, 310027, China
*Corresponding author, e-mail: farman.mangi@salu.edu.pk

Abstract

A fission transmission linear-to-circular polarization conversion based on bi-layer structure is proposed which is composed of 3 × 3 array to convert linear-to-circular polarized wave. The structure is constructed by half square with "H" shape printed on both sides of the dielectric substrate that are subjected to obtain multi-band at resonance frequencies. The proposed structure realizes the giant circular polarization under the normal incidence for right and left circular polarized waves. After transmission, the incident wave decomposed into two orthogonal linear components have equal magnitudes and 90o phase difference between them. The novel approach of "fission transmission of electromagnetic waves" is firstly introduced to understand the physics of giant circular polarization conversion which is based on the sequence of incident and transmitted waves to generate strong circular dichroism.

Keywords*: asymmetric transmission, circular polarization, multi-band circular polarizer, metamaterial, bquarter wave plate*

1. Introduction

Polarization is a basic characteristics of EM waves, which is widely used in various EM wave applications including radar, and wireless communication system. Polarizer is an important method to realize circular polarization wave. Circular polarizer can transfer the linear-to-circular polarized wave under the normal incidence of plane wave. Circular polarizer can be designed by employing photonic [1-3], chiral structures [4-8], metasurface, metamaterials [9], meander-line [10], slots of different structures [11,1 2], waveguide [13, 14], grating structures [15, 16], quarter wave plate [17, 18], etc.

The layer-by-layer chiral metamaterial structure was presented to achieve circular dichroism and exhibit the characteristics of two-dimensional and three-dimensional structures [19]. The concept of bi-layered chiral metamaterial were presented to enhance the asymmetric transmission for circular polarized wave. It was observed that the magnitude of asymmetric transmission parameter based on the distance between metal layers [20].

Another contribution of an ultrathin asymmetric chiral metamaterial multi-band structure composed of twisted double-gap spilt resonator was introduced in which the large polarization extension ratio of more than 18 dB was achieved at four resonant frequencies [21]. A bi-layer twisted spilt-ring structure asymmetric chiral metamaterial was presented to achieve circularly polarized wave with dual bands. The proposed dual-band structure features high conversion efficiency at resonant frequencies. In addition, the large polarization extension ratio of more than 16 dB was obtained [22].

The double-layer spilt ring resonator structure was proposed which obtain the pronounced circular dichroism effect in addition to RHCP wave and LHCP wave [23]. A kind of circular polarizer convertor based on bi-layered asymmetrical spilt ring metamaterial was proposed which convert RHCP wave to LHCP wave and optimize the circular polarizer by varying the distance between two metal layers [24]. The simple bilayer structure was proposed as near-perfect dual-band circular polarizer based on bilayer twisted. The presented structure

Received April 2, 2016; Revised July 25, 2016; Accepted August 10, 2016

obtained the RHCP wave and LHCP wave, which exhibits the polarization extension ratio more than 30 dB at operated frequencies [25].

Multilayer structures are introduced for FSSs to manipulate the polarization state. Wideband circular polarizer is proposed using stacked dual-layer periodic arrays [26], which are separated by large distance of 0.33 operational wavelength. As shown in [27], the performance of circular polarizers can be improved by using multilayers, but the fabrication becomes expensive and challenging because they contain up to multilayers. The multi-band of polarizer is useful for many applications. The polarization characteristics of transmitted wave of dual-band asymmetry chiral metamaterial structure was demonstrated in [28].

A proposed fission transmission linear-to-circular polarization converter based on compact bi-layer is presented. The transmission characteristics of T_{xx} and T_{xy} of the proposed structure is investigated on the four frequency bands. The novel approach of "fission transmission of electromagnetic waves" is firstly introduced to obtain strong circular dichroism based on the incident of linearly polarized wave which is converted into two orthogonal components through lower printed metallic strips layer. Simultaneously, the two transmitted orthogonal components impinges on the upper printed strips along +z direction and converted into four orthogonal vector components at the end of structure. In order to sequence of projection and transmission of orthogonal components through printed structure produce strong circular dichroism. Meanwhile, the sequence of projection and transmission result strong magnetic response between two layers. In order to realize this idea, the distribution of surface currents are analyzed to demonstrate the strong circular polarization conversion. The designed structure achieves two orthogonal polarization eigenstates (RHCP) wave and (LHCP) wave at four frequency bands. The significant advantages of this proposed structure are obtained, such as, multi-broadband, good circular polarization, simple and compact structure, easy fabrication and can be used for the microwave applications.

2. Structure Design

Figure 1 depicts the unit cell of compact multi-band circular polarizer. The two structure with same size are printed both sides of substrate with different directions in XOY plane. The top printed structure is tilted at 45^o and the bottom slanted at -45^o along xoy directions, respectively. The substrate is chosen with relative permittivity εr and thickness *t*. The length and the width of the structure are represented by l_1, l_2, l_3 and w_1, w_2, respectively, whereas, the thickness of structure is assumed to be negligible as compare to operational wavelength. The periods of the unit cell are represented by *px* and *py* in x and y sides.

The software ANSYS HFSS is used to simulate the unit cell and get the electromagnetic characteristics. The dielectric substrate Roger RT/duroid 5880 is employed in this design. The selected parameters are as εr=2.2 with loss tangent of 0.0009, *t* = 0.787 mm, l_1 = 1.13 mm, l_2 = 2.26 mm, l_3 = 1.41 mm, w_1 = 0.35 mm, w_2 = 0.35 mm, *px* = 5mm and *py* = 5 mm, respectively as shown in Figure 1(a). The periodic boundary conditions Master and Slave are assigned to simulate the infinitely periodic geometrical structure along x and y axis. The excitation of port1 and port 2 is provided by floquet modes with two orthogonal waves represent the vertically (E_x) and horizontally (E_y) polarized vector components of the incident wave.

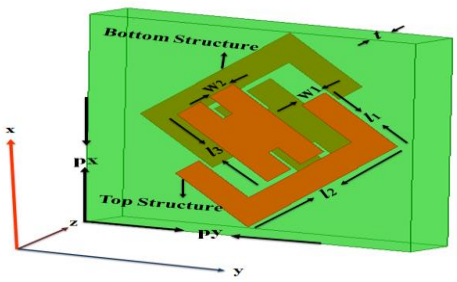

Figure 1. Geometry of the Unit Cell of Compact Multi-Band Circular Polarizer

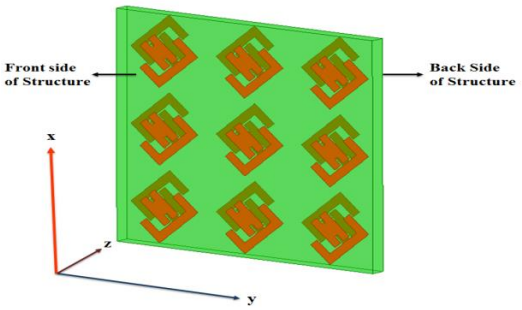

Figure 2. Simulation Model of Compact Multi-band Circular Polarizer based on 3x3 Array

We proposed periodical 3 × 3 array of identical units printed on top and bottom sides of the substrate depicted in Figure 2. The array occupies an overall area of 15mm × 15mm. The bottom tilted structure pattern is formed by rotating an enantiometric form of the upper slanted strips pattern by 90°. The periodical absorbing boundary conditions are used around the infinitely 3 × 3 array simulated model and open boundary conditions are applied along the perpendicular to the direction of EM wave propagation. An incident linearly polarized wave can be decomposed into two orthogonal vector components which pass through polarizer with different velocities; the outgoing field is circular polarized wave at the end of polarizer.

3. Operating Principle

The circularly polarization purity depends in structure of the proposed multi-band circular polarizer. Assuming the beam of x-polarized wave is impinged along +z direction, the incident wave can be expressed as:

$$E_i = E_x = \hat{x} E_0 e^{ik_z z} \tag{1}$$

When the structure is excited by polarized wave the transmitted electric field is determined as:

$$E_t = \hat{x} T_{xx} E_i + \hat{y} T_{xy} E_i \tag{2}$$

The RHCP and LHCP transmitted waves are achieved when the amplitudes of T_{xy} and T_{xx} equal to each other. The transmitted RHCP wave and LHCP wave can be expressed as:

$$E_{RHCP} = T_{RHCP-x}\left(\frac{\sqrt{2}}{2}(E_i \hat{x} + E_i e^{i\frac{\pi}{2}} \hat{y})\right) \tag{3}$$

$$E_{LHCP} = T_{LHCP-x}\left(\frac{\sqrt{2}}{2}(E_i e^{i\frac{\pi}{2}} \hat{x} + E_i \hat{y})\right) \tag{4}$$

It is expressed that $T_{xx} = E_x^t/E_x^i$, $T_{xy} = E_y^t/E_x^i$. In these expressions, the first subscript indicates the output polarized wave and second subscript represents the input signal polarizations, respectively. For instance,$T_{xy} = E_y^t/E_x^i$, where E_x^i is the applied as input x-polarized wave along +z direction and E_y^t is transmitted y-component of electric field. The complex transmission and reflection can be defined as $T_{\pm} = T_{xx} \pm i$, T_{xy} where "+" and "–" refer to the right- and left-handed circular polarization [29].

It is defined that the normally incident electric field is along -x direction, the transmission of co-polarization $T_{xx}$and cross polarization T_{xy}can be evaluated, where the first subscript represents the polarization of transmitted field and second subscript represents the polarization of incident field. If the cross-polarization is lower than co-polarization T_{xx}<T_{xy}, it means that transmitted waves are elliptic polarization. Therefore, the co- and cross-polarization transmission coefficients should have equal amplitudes and phase difference between them must be $\eta\pi/2$.

Assuming that $T_{xx} = E_x^t/E_x^i$ represent the transmittance of x-to-x and x-to-y polarization conversions. The two decomposed components of transmitted linearly polarized waves E_x^t and E_y^t from the bottom layer employ as incident polarized waves E_x^i and E_y^i for the top layer along the +z direction. As, the incidence of E_x^i and E_y^i as the excitation source, the two more pairs of orthogonal vector components can be generated at the other side of top layer, which realize the novel approach of "fission yields vector components of electromagnetic waves".

Moreover, the high polarization conversion efficiency and asymmetric transmission is achieved through proposed structure based on bi-layer structure. Subsequently, it is realized

that four transmitted orthogonal vector components converge to each other and constitute strong circular dichroism at the end of structure. The physics of operating principle based on the fission transmission of electromagnetic waves which realizes the incident wave decompose into two transmitted wave through bottom layer and output two orthogonal wave impinges on the surface of upper layer to be converted into four transmitted orthogonal components at the end of structure. Moreover, it is assumed that the sequence of an incident and transmission products causes additional transmission of orthogonal components to sustain chain transmission of EM waves by using double metallic layered structure.

4. Result and Discussion

Initially, numerical simulation is used to better understanding the polarization conversion and transmission characteristics of unit cell structure by using ANSYS HFSS. The incident x-linearly polarized wave is employed as excitation source to the sample surface. The model is excited by floquet port1 with linearly polarized wave range from 25-40 GHz. Figure 3 represents the transmission coefficients of T_{xx} and T_{xy} under the normal incidence of electric field. The transmission coefficients of T_{xx} are 2.71 dB, (f1 = 32.58GHz), and 5.73 dB (f2 = 37.18GHz), respectively. Meanwhile, the transmission coefficients of T_{xy} are obtained 3.95 dB at (f1) and 4.89 dB at (f2), respectively. In order to achieve polarization conversion of transmitted waves, the axial ratio $AR = |T_{xy}|/|T_{xx}|$ and their phase differences $\Phi(|T_{xy}|) - \Phi(|T_{xx}|)$ of cross- polarization and co-polarization transmission are achieved.

The axial ratios between transmitted waves T_{xx} and T_{xy} are shown in Fig.4, and the corresponding phase differences results between transmitted waves are presented in Fig. 5 which attributes the values of phase difference at the operated frequency bands. Where, the values of axial ratios are 1.2 at (f1) and 1.1 at (f2), respectively. The corresponding phase differences are calculated to be 90.81^{o} at (f1), and 127^{o} at (f2), which means purely circularly polarized wave are achieved at distinct frequency bands.

Figure 4 represents the large axial ratio bandwidths at two frequency bands ranging from 25GHz-40GHz, which are contained at 31.29–33.04GHz, BW = 5.38% and 37.04–37.22 GHz, BW=0.55% , respectively. The accumulated axial ratio bandwidth of 5.93% is obtained at the dual-band ranging from 25GHz-40GHz. The RHCP wave is obtained at dual band. In general, the polarization azimuth ratio is expressed by ϕ = (arg (T+) − arg (T−))/2 to calculate the polarization changes of the structure.

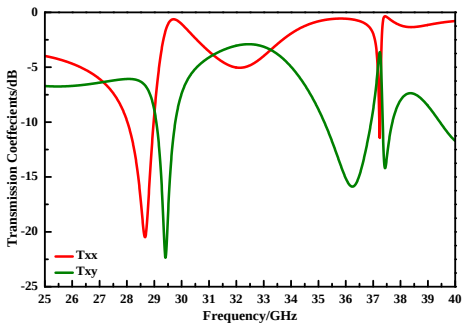

Figure 3. Indicates the transmission coefficients of Txx and Txy versus frequency for normal incident wave at θ = 0o

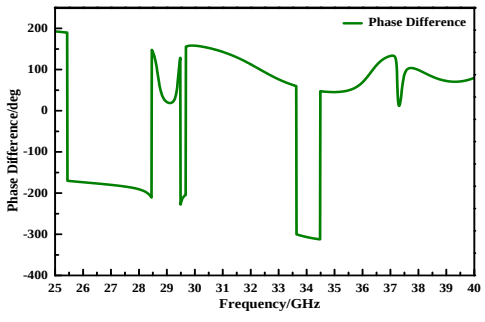

Figure 4. Represents the Phase Difference Between Transmitted Wave Versus Frequency

Figure 6 represents the transmission coefficients of T_{xx} and T_{xy}. The transmission coefficients of Txx are 10.82 dB (f1 = 30.24GHz), 5.28 dB (f2 = 33.90GHz), 5.49 dB (f3 = 35.40 GHz) and 7.29 dB (f4 = 38.82 GHz), respectively. Meanwhile, the transmission coefficients of Txy are obtained 10.57 dB (f1), 8.71 dB (f2), 10.35 dB (f3), and 7.71 dB (f4), respectively.

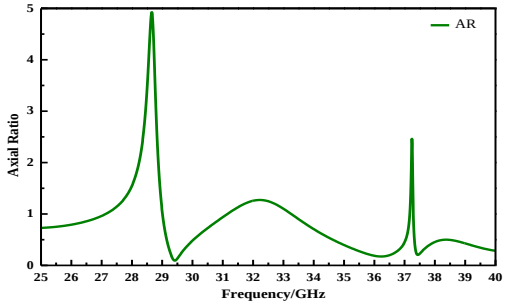

Figure 5. Denotes the Axial Ratio of Transmitted Wave Versus Frequency

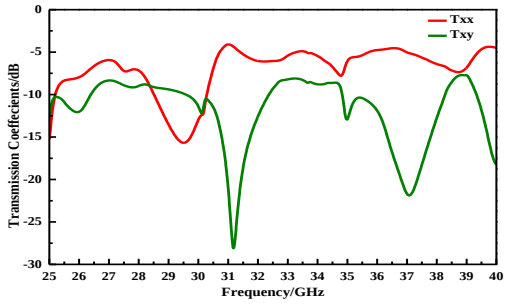

Figure 6. Indicates the transmission coefficients of T_{xx} and T_{xy} versus frequency for normal incident wave at $\theta = 0^{o}$

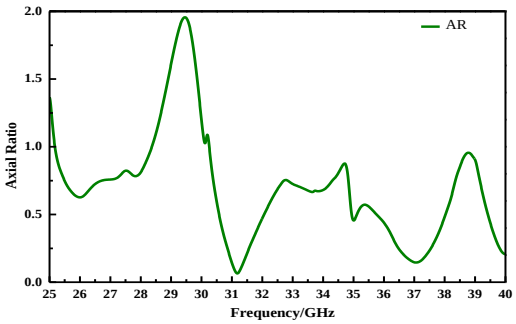

Figure 7. Denotes the Axial Ratio of Transmitted Wave Versus Frequency

The axial ratios between transmitted waves are shown in Figure 7 and the corresponding phase differences results are presented in Figure 8 which attributes the values of phase difference at the operated frequency bands. Where, the values of axial ratio are 1.02, 0.67, 0.57, and 0.95, respectively. The corresponding phase differences are calculated to be -135.33^{o} (f1), -90.39^{o} (f2), -122.07^{o} (f3) and 255.31^{o} (f4), respectively.

Figure 8 represents the large axial ratio bandwidth at the four different resonances ranging from 25GHz-40GHz, which are broaden at 29.47–30.24GHz, BW= 2.36%, 32.90–34.83GHz, BW = 5.93%, 35.12–35.75GHz, BW = 1.95% and 38.46–39.18GHz, BW = 2.21%, respectively. It is shown that the accumulated axial ratio bandwidth of 12.45% is obtained at the four corresponding frequency bands ranging from 25GHz-40GHz. The generated outgoing wave are RHCP and LHCP waves are assumed that polarizer is illuminated by the incident wave polarized at slant 45o and -45o, respectively. The RHCP waves are obtained at 30.90.47-33.74 GHz, 38.80-39.18 GHz and LHCP wave are achieved at 29.47-30.24 GHz, 33.75-34.84 GHz, 35.12-35.75 GHz and 38.46-38.79 GHz, respectively. In order to evaluate the performance of multi-band compact circular polarizer by using the polarization conversion coefficient corresponding phase difference over four broadband resonant frequencies under the normal incident angle.

To elucidate the physical origin of strong circular dichroism and optical activity of our design, the surface current distribution can be observed on top and bottom structure printed on both sides of substrate at the resonant frequencies, as depicted in Figure 4. The solid (dash) line arrows indicates the front (back) surface current distribution and electric field direction on the top and bottom strips. The surface currents are in same directions on front and back side of structure at 30.24 GHz and 38.82 GHz which attributing to symmetric resonance mode. Meanwhile, the, surface currents on the top and bottom layers are in opposite direction on both sides of structure at 33.90 GHz and 35.40 GHz which corresponds to an asymmetric resonance mode. It means that the surface currents indicate the excitation of giant circular dichroism effect

of frequencies 30.24 GHz and 38.82 GHz results from the electric dipole resonance, and two frequencies 33.90 GHz and 35.40 are mainly from the magnetic dipole resonance.

From Figure 4(a) and (b), it can be observed that the surface currents direction on the top and bottom strips are antiparallel at all distinct resonant frequencies, which shows the effective current loops. It is realized that the magnetic vectors induced by current loops on the surface of the strips are not perpendicular to the electric vectors of the incident wave, therefore, the cross-coupling behaviour between electric and magnetic fields realizes at four resonant frequencies. Similarly, the surface current distribution at some portion of the layers is week because the magnetic field is parallel to the y-direction and electric field along x -direction, resulting in the transmitted cross-polarized wave. Based on the fact that the direction of surface currents between two layers create electromagnetic response is shown as black arrows:

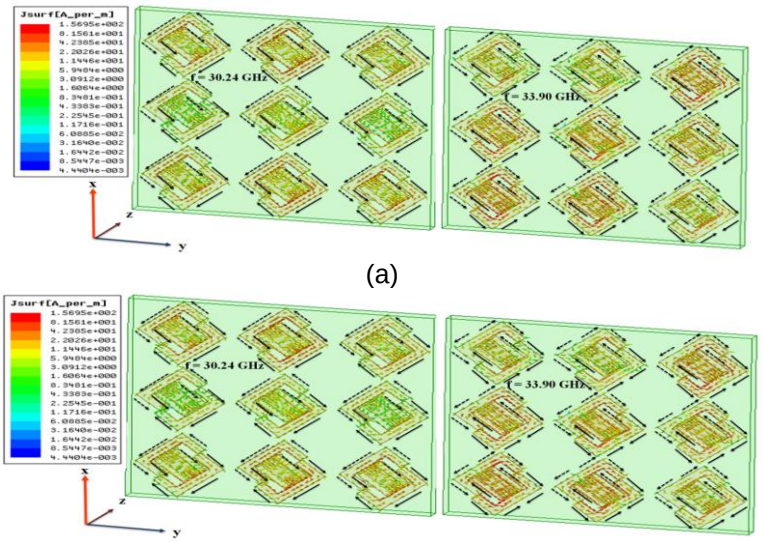

Figure 4. (a) and (b) Shows the Distributions of Surface Currents on Top and Bottom Structure Printed on Both Sides of Substrate Under the Incident Field with E in the x Direction Propagating Along +z Direction at (a) f = 30.24 GHz, (b) f = 33.90 GHz, (c) f = 35.40 GHz, and (d) f = 38.82 GHz

Figure 4(a) and (b) represent the direction of currents which are totally antiphase between two layers and attributes the giant circular polarization conversion at distinct frequencies. Whereas, the in-phase currents represent the electric response and antiphase can lead to magnetic response [30-33]. The incident x-polarized wave excites the current loops in metallic strips which produces the magnetic dipole moment. In addition, the electric and magnetic responses exists not only on the surface of the each strips but also between the strips due to the strong coupling effect [34, 35].

5. Conclusion

In summary, the proposed structure is comprehensively characterized with good transmission of decomposed orthogonal vector components. Firstly, the novel concept of “fission transmission of EM waves” is introduced and its physics to realize the strong circular dichroism at resonant frequencies. This novel approach can be realized by employing multi-layers to achieve strong optical activity at frequency bands. The performance of multi-band circular polarizer is computed with HFSS simulation. The proposed structure has good circular polarization efficiency, multi-broadband operating bandwidth which makes potentially useful for many practical systems. The designed model of polarizer is compact, very simple and can be easily fabricated. Moreover, it is possible to enhance the bandwidth performance by changing

some geometric parameters of the circular polarizer, such as, thickness of substrate, size, orientation of strips and using multi-layer to obtain giant circular dichroism.

Acknowledgements

Mr. Farman Ali Mangi, Mr. Shaoqiu Xiao and Ghulam Ali Mallah proposed this idea and constructed methods for this research. Miss. Ghulam Fatima Kakepoto worked on the designed simulation models and collected the related literature review. A proof of concepts and determination of reported designs were completed by Mr. Imran Memon. All authors read and approved the final manuscript.

Funding

This work was supported in part by National Natural Science Foundation of China under Grant 61271028, 61271027 and 61101039, in part by Fok Ying Tong Education Foundation under Grant 131107 and in part by Research Fund for the Doctoral Program of Higher Education of China under Grant 20130185110024.

References

[1] JK Gansel, M Thiel, MS Rill, M Decker, K Bade, V Saile, G von Freymann, S Linden, M Wegener. Gold helix photonic metamaterial as broadband circular polarizer. *Science.* 2009; 325(5947): 1513-1515.
[2] J Kaschke, JK Gansel, M Wegener. On metamaterial circular polarizers based on metal N-helices. *Opt. Express,* 2012; 20(23): 26012-26020.
[3] YF Li, JQ Zhang, SB Qu, JF Wang, HY Chen, Z Xu, AX Zhang. Wideband selective polarization conversion mediated by three-dimensional metamaterials. *J. Appl. Phys*. 2014; 115(23): 234-506.
[4] XJ Huang, D Yang, HL Yang. Multiple-band reflective polarization converter using U-shaped metamaterial. *J. Appl. Phys.* 2014; 115(10): 103-505.
[5] Y Huang, Y Zhou, ST Wu. Broadband circular polarizer using stacked chiral polymer films. *Opt. Express*. 2007; 15(10): 6414–6419.
[6] HX Xu, GM Wang, MQ Qi, T Cai, TJ Cui. Compact dual-band circular polarizer using twisted Hilbert-shaped chiral metamaterial. *Opt. Express*. 2013; 21(21): 24912–24921.
[7] M Mutlu, AE Akosman, AE Serebryannikov, E Ozbay. Asymmetric chiral metamaterial circular polarizer based on four U-shaped split ring resonators. *Opt. Lett.* 2011; 36(9): 1653–1655.
[8] S Yan, GAE Vandenbosch. Compact circular polarizer based on chiral twist double split-ring resonator. *Appl. Phys. Lett.* 2013; 102(10): 103503.
[9] HL Zhu, SW Cheung, KL Chung, TI Yuk. Linear-to-circular polarization conversion using metasurface. *IEEE Trans. Antenn. Propag*. 2013; 61(9): 4615-4623.
[10] RS Chu, KM Lee. Analytical model of a multilayered meander-line polarizer plate with normal and oblique plane-wave incidence. *IEEE Trans. Antenn. Propag*. 1987; 35(6): 652–661.
[11] M Euler, V Fusco, R Dickie, R Cahill. Comparison of frequency-selective screen-based linear to circular split-ring polarization convertors. *IET Microwave Antennas Propag.* 2010; 4(11): 1764-1772
[12] J Wang, Z Shen. Improved polarization converter using symmetrical semi-ring slots. *IEEE Antennas Propag. Society Int. Symp*. 2014: 2052–2053.
[13] E Lier, TS Pettersen. A novel type of waveguide polarizer with large cross-polar bandwidth. *IEEE Trans. Microw. Theory Tech*. 1988; 36(11): 1531–1534.
[14] SW Wang, CH Chien, CL Wang, RB Wu. A circular polarizer designed with a dielectric septum loading. *IEEE Trans. Microw. Theory Tech.* 2004; 52(7): 1719-1723.
[15] M Mutlu, AE Akosman, E Ozbay. Broadband circular polarizer based on high-contrast gratings. *Opt. Lett*. 2012; 37(11): 2094–2096.
[16] M Mutlu, AE Akosman, G Kurt, M Gokkavas, E Ozbay. Experimental realization of a high-contrast grating based broadband quarter-wave plate. *Opt. Express.* 2012; 20(25): 27966-27973.
[17] M Joyal, J Laurin. Analysis and design of thin circular polarizers based on meander lines. *IEEE Trans. Antennas Propag*. 2012; 60(6): 3007–3011.
[18] Carl Pfeiffer, Anthony Grbic. Millimeter-Wave Transmit arrays for Wave front and Polarization Control. *IEEE Transactions on Microwave Theory and Techniques*. 2013; 61(12): 4407.
[19] Wu Lin, ZhenYu Yang, YongZhi Cheng, ZeQin Lu, Peng Zhang, Ming Zhao, RongZhou Gong, XiuHua Yuan, Yu Zheng, JiAn Duan. Electromagnetic Manifestation of Chirality in Layer-by-Layer Chiral Metamaterials. *Optics express*. 2013; 21(5): 5239-5246.

[20] Lin Wu, ZhenYu Yang, Ming Zhao, Peng Zhang, ZeQing Lu, Yang Yu, ShengXi Li, Xiu Hua Yuan. Giant Asymmetric Transmission of Circular Polarization in Layer-by-Layer Chiral Metamaterials. *Applied Physics Letters*. 2013; 103: 021903.
[21] W Yuan, H Zhang, Y Cheng. *Asymmetric Chiral Metamaterial Multi-Band Circular Polarizer Based on Combined Twisted Double-Gap Split-Ring Resonators.* Progress In Electromagnetics Research Conference. 2014; 49: 141-147.
[22] Yong Zhi Cheng, Yie Nie, Zheng Ze Cheng, Rong Zhou Gong. Dual-Band Circular Polarizer and Linear Polarization Transformer Based on Twisted Split-Ring Structure Asymmetric Chiral Metamaterial. *Progress in Electromagnetics Research*. 2014; 145: 263-272.
[23] Y Cheng, Y Nie, L Wu, RZ Gong. Giant Circular Dichroism and Negative Refractive Index of Chiral Metamaterial Based on Split-Ring Resonators. *Progress In Electromagnetics Research*. 2013; 138, 421-432.
[24] Cheng, Yongzhi, Rongzhou Gong, Zhengze Cheng, Yan Nie. Perfect Dual-Band Circular Polarizer Based on Twisted Split-Ring Structure Asymmetric Chiral Metamaterial. *Applied Optics.* 2014; 53(25): 5763-5768.
[25] M Euler, V Fusco, R Dickie, R Cahill. Comparison of frequency-selective screen-based linear to circular split-ring polarization convertors. *IET Microwave Antennas Propag.* 2010; 4(11), 1764-1772.
[26] RS Chu, KM Lee. Analytical model of a multilayered meander-line polarizer plate with normal and oblique plane-wave incidence. *IEEE Trans. Antenn. Propag.* 1987; 35(6): 652–661.
[27] Xiaoliang Ma, Cheng Huang, Mingbo Pu, Yanqin Wang, Zeyu Zhao, Changtao Wang, Xiangang Luo. Dual-band asymmetry chiral metamaterial based on planar spiral structure. *Appl. Phys. Lett.* 2012; 101: 161901.
[28] Sen Yan, Guy AE Vandenbosch. Compact circular polarizer based on chiral twisted double split-ring resonator. *Appl. Phys. Lett.* 2013; 102: 103503.
[29] Z Wu, BQ Zeng, S Zhong. A Double-Layer Chiral Metamaterial With Negative Index. *J. of Electromagn. Waves and Appl*. 2010; 24: 983-992.
[30] R Singh, IAI Ai-Naib, M Koch, WL Zhang. Sharp Fano resonances in THz metamaterials. *Opt. Express*. 2011; 19: 6312–6319.
[31] JH Shi, Z Zhu, HF Ma, WX Jiang, TJ Cui. Tunable symmetric and asymmetric resonances in an asymmetrical split-ring metamatrial. *J. Appl. Phys.* 2012; 112: 073522
[32] Y Ye, S He. 90° polarization rotator using a bilayered chiral metamaterial with giant optical activity. *Appl. Phys. Lett.* 2010; 96: 203501.
[33] C Huang, X Ma, M Pu, G Yi, Y Wang, X Luo. Dual-band 90° polarization rotaor using twisted split ring resonators array. *Opt. Commun*. 2013; 291: 345–348.
[34] Y Ye, S He. 90° polarization rotator using a bilayered chiral metamaterial with giant optical activity. *Appl. Phys. Lett.* 2010; 96: 203501.
[35] C Huang, X Ma, M Pu, G Yi, Y Wang, X Luo. Dual-band 90° polarization rotaor using twisted split ring resonators array. *Opt. Commun*. 2013; 291: 345–348.